

SCIENTIFIC REPORTS



OPEN

One-step resonant controlled-phase gate on distant transmon qutrits in different 1D superconducting resonators

Ming Hua^{1,2,3,4,*}, Ming-Jie Tao^{4,*}, Fu-Guo Deng^{4,*} & Gui Lu Long^{1,2,3,*}

Received: 29 April 2015
Accepted: 27 August 2015
Published: 21 October 2015

We propose a scheme to construct the controlled-phase (c-phase) gate on distant transmon qutrits hosted in different resonators inter-coupled by a connected transmon qutrit. Different from previous works for entanglement generation and information transfer on two distant qubits in a dispersive regime in the similar systems, our gate is constructed in the resonant regime with one step. The numerical simulation shows that the fidelity of our c-phase gate is 99.5% within 86.3 ns. As an interesting application of our c-phase gate, we propose an effective scheme to complete a conventional square lattice of two-dimensional surface code layout for fault-tolerant quantum computing on the distant transmon qutrits. The four-step coupling between the nearest distant transmon qutrits, small coupling strengths of the distant transmon qutrits, and the non-population on the connection transmon qutrit can reduce the interactions among different parts of the layout effectively, which makes the layout be integrated with a large scale in an easier way.

Universal quantum gate is the key element for quantum computation^{1–9}. Two-qubit universal controlled-phase (c-phase) gate, the equivalent of two-qubit controlled-not (CNOT) gate (or the hyper-parallel two-photon CNOT gates on photon systems with two degrees of freedom^{7–9}), can form universal quantum computing assisted by single-qubit operations, and it has attracted much attention in recent years. To realize the deterministic quantum entangling gates, nonlinear interactions on qubits are required. Cavity quantum electrodynamics (QED)¹⁰ provides a promising platform to realize the nonlinear interaction between an atom and a field, and it can achieve indirect nonlinear interaction among atoms or fields. To simulate cavity QED, atom^{11–13}, spin^{14–25}, or superconducting qubits^{26–36} coupled to optical cavities^{37–41}, superconducting resonators^{42–45}, or nanomechanical resonators^{46,47} have been studied a lot for quantum information processing both in experiment and in theory⁴⁸.

Circuit QED, composed of a superconducting qubit coupled to a superconducting resonator^{42,43}, gives a powerful candidate platform for quantum computation⁴⁹ because of large-scale integration of superconducting qubits and all-electrical control using standard microwave and radio-frequency engineering techniques. It can work from the dispersive weak regime to the resonant strong regime⁵⁰, and even the ultra-strong regime⁵¹. In microprocessors based on circuit QED, there are some interesting types of integration of superconducting qubits or resonators for quantum information processing, including several qubits coupled to a resonator^{52–54}, several resonators coupled to a qubit or several qubits^{55–64}, or some circuit QED systems coupled to each other by using qubits, superconducting transmission lines,

¹State Key Laboratory of Low-Dimensional Quantum Physics and Department of Physics, Tsinghua University, Beijing 100084, China. ²Tsinghua National Laboratory for Information Science and Technology, Beijing 100084, China. ³Collaborative Innovation Center of Quantum Matter, Beijing 100084, China. ⁴Department of Physics, Applied Optics Beijing Area Major Laboratory, Beijing Normal University, Beijing 100875, China. *These authors contributed equally to this work. Correspondence and requests for materials should be addressed to G.L.L. (email: gllong@tsinghua.edu.cn)

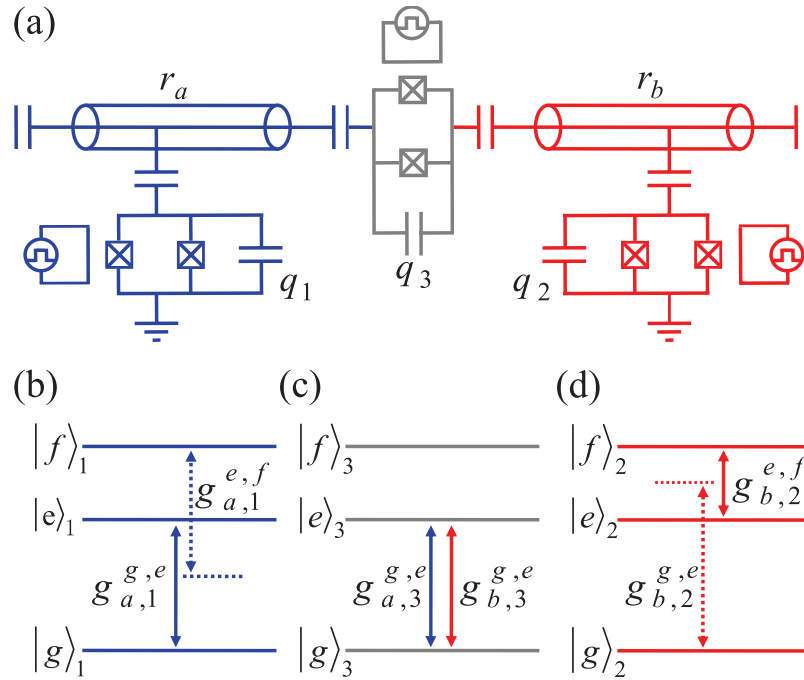


Figure 1. (a) The setup for the construction of our c-phase gate on the distant transmon qutrits q_1 and q_2 . q_1 (q_2) is coupled to the high-quality resonator r_a (r_b). The two resonators are interconnected by a connection transmon qutrit q_3 . (b–d) are the illustrations of interactions between q_1 and r_a , q_3 and r_a (r_b), and q_2 and r_b , respectively.

or capacitance^{65–69}. The basic tasks of quantum computation in circuit QED have been demonstrated in experiment, such as the c-phase gate^{52,70–72} and the controlled-controlled-phase gate^{53,54} on transmon qubits in the processor by integrating several superconducting qubits coupled to a 1D superconducting resonator, the generation of the entangled states on transmon qubits⁷³ or two resonator qutrits⁶⁰, and the measurement on superconducting qubits^{69,74} or the microwave photons in a superconducting resonator^{75–78}.

To avoid the indirect interaction among qubits in the processor by integrating more superconducting qubits coupled to a 1D superconducting resonator for complex quantum computation, one should take much smaller coupling strength between a qubit and the resonator or tunable coupling qubits. To integrate more resonators coupled to a qubit, smaller or tunable coupling between the qubit and each resonator is required as well. Small coupling strength leads to a slow quantum operation which limits the performance of the quantum computation due to the coherence time of qubits and decay rate of resonators. Tunable coupling between a qubit and multiple resonators increases the difficulty to design the superconducting circuits. As another candidate for integration of large-scale quantum computation, superconducting qubits hosted in different resonators interconnected by a qubit has been studied in experimental and theoretic works^{67,71}. Up to now, there are no schemes to construct the multi-qubit universal gates on the distant transmon qubits in the similar systems.

In this paper, we propose a scheme to complete the c-phase gate on two distant transmon qutrits (DTQs) hosted in different resonators interconnected by a connection transmon qutrit (CTQ). Different with the schemes for entanglement generation and information transfer in the similar device⁶⁷, our c-phase gate on two DTQs is achieved with one step by taking the same frequencies of qutrits and resonators and small coupling strengths of DTQs. Finally, we discuss the feasibility about its possible experiment implementation with the similar systems in previous works^{70,71} and construct a conventional two-dimensional surface code (SC) layout^{79,80} as an interesting possible application of our c-phase gate. Although our layout needs extra CTQs than the one in the previous work⁷⁰, there is almost no demand on the life time of the CTQ as the information does not be populated in it during the gate operation, and the interactions between nearest DTQs are reduced into four-step coupling. On one hand, the small coupling strength of DTQs can reduce the interactions between a qutrit and the nearest resonators. On the other hand, four-step coupling between nearest DTQs can be turned on and off easily by CTQs. These characters make our layout suitable to be integrated with a large scale.

Results

C-phase gate on distant transmon qutrits. Let us consider a system composed of two DTQs coupled to different superconducting resonators interconnected by a CTQ, shown in Fig. 1. The Hamiltonian of the system in the interaction picture is ($\hbar = 1$)

$$H^{cp} = \sum_{I=1,3} \left(g_{a,I}^{g,e} a \sigma_{I;g,e}^+ e^{i\delta_{a,I}^{g,e} t} + g_{a,I}^{e,f} a \sigma_{I;e,f}^+ e^{i\delta_{a,I}^{e,f} t} \right) + \sum_{J=2,3} \left(g_{b,J}^{g,e} b \sigma_{J;g,e}^+ e^{i\delta_{b,J}^{g,e} t} + g_{b,J}^{e,f} b \sigma_{J;e,f}^+ e^{i\delta_{b,J}^{e,f} t} \right) + h.c. \quad (1)$$

Here, a and b are the annihilation operators of the resonators r_a and r_b , respectively. $\sigma_{I(J);g,e}^+$ and $\sigma_{I(J);e,f}^+$ are the creation operators of the transitions $|g\rangle_{I(J)} \leftrightarrow |e\rangle_{I(J)}$ and $|e\rangle_{I(J)} \leftrightarrow |f\rangle_{I(J)}$ of $q_{I(J)}$, respectively. $g_{a(b),I(J)}^{g,e}$ and $g_{a(b),I(J)}^{e,f}$ are the coupling strengths between the two transitions of $q_{I(J)}$ and $r_{a(b)}$, respectively. $\delta_{a(b),I(J)}^{g,e} = \omega_{I(J)}^{g,e} - \omega_{a(b)}$ and $\delta_{a(b),I(J)}^{e,f} = \omega_{I(J)}^{e,f} - \omega_{a(b)}$. $\omega_{I(J)}^{g,e}$ ($\omega_{I(J)}^{e,f}$) is the transition frequency between the states $|g\rangle_{I(J)}$ and $|e\rangle_{I(J)}$ ($|e\rangle_{I(J)}$ and $|f\rangle_{I(J)}$) of the qutrit $q_{I(J)}$. $\omega_{a(b)}$ is the frequency of the resonator $r_{a(b)}$. $|g\rangle$ is the ground state of a transmon qutrit, and $|e\rangle$ and $|f\rangle$ are the first and the second excited states, respectively.

In order to obtain the effective Hamiltonian of the system composed of the two resonators (r_a and r_b) and three superconducting qutrits (q_1 , q_2 , and q_3) to construct our c-phase gate, we take small values of $g_{a,1}^{g,e}$, $g_{a,1}^{e,f}$, $g_{b,2}^{g,e}$, and $g_{b,2}^{e,f}$ with $g_{a(b),1(2)}^{g,e(e,f)} \ll |\omega_{1(2)}^{g,e} - \omega_{1(2)}^{e,f}|$ and $\omega_1^{g,e} = \omega_2^{e,f} = \omega_a = \omega_b = \omega_3^{g,e}$ to make the transitions $|e\rangle_1 \leftrightarrow |f\rangle_1$ of q_1 and $|g\rangle_2 \leftrightarrow |e\rangle_2$ of q_2 to detune largely with r_a and r_b , respectively, which indicates the dispersive coupling between the transition $|e\rangle_1 \leftrightarrow |f\rangle_1$ and r_a and that between $|g\rangle_2 \leftrightarrow |e\rangle_2$ and r_b can be ignored. Besides, only the transition $|g\rangle_3 \leftrightarrow |e\rangle_3$ of the CTQ q_3 should be considered as the coupling is the dispersive one and there is just one microwave photon can be generated in the resonators (just the transitions $|g\rangle_1 \leftrightarrow |e\rangle_1$ of q_1 and $|e\rangle_2 \leftrightarrow |f\rangle_2$ of q_2 are used in our scheme), respectively. Here, the Hamiltonian can be reduced from Eq. (1) to

$$H_1^{cp} = g_{a,1}^{g,e} (a \sigma_{1;g,e}^+ + a^+ \sigma_{1;g,e}^-) + g_{b,2}^{e,f} (b \sigma_{2;e,f}^+ + b^+ \sigma_{2;e,f}^-) + g_{a,3}^{g,e} (a \sigma_{3;g,e}^+ + a^+ \sigma_{3;g,e}^-) + g_{b,3}^{g,e} (b \sigma_{3;g,e}^+ + b^+ \sigma_{3;g,e}^-). \quad (2)$$

To our purpose, we then take the transformations $a = \frac{1}{2}(c_+ + c_- + \sqrt{2}c)$, $b = \frac{1}{2}(c_+ + c_- - \sqrt{2}c)$, and $\sigma_{3;g,e}^- = \frac{\sqrt{2}}{2}(c_+ - c_-)$ with the condition $\{g_{a,3}^{g,e}, g_{b,3}^{g,e}\} \gg \{g_{a,1}^{g,e}, g_{b,2}^{e,f}\}$ and $g_{a,3}^{g,e} = g_{b,3}^{g,e} = g^{81-83}$. The transformations give us three new normal modes and only one of them (that is, c) resonates with the qutrits, so we can ignore the other two detuning modes and the system is reduced to a two-qubit one resonantly coupled to a single mode of the resonant field (further details can be found in the method). Eq. (2) becomes

$$H_{eff}^{cp} = \frac{1}{\sqrt{2}} [g_{a,1}^{g,e} (c \sigma_{1;g,e}^+ + c^+ \sigma_{1;g,e}^-) - g_{b,2}^{e,f} (c \sigma_{2;e,f}^+ + c^+ \sigma_{2;e,f}^-)]. \quad (3)$$

Here, the frequencies of c mode and c_{\pm} mode are $\omega_{a(b)}$ and $\omega_{a(b)} \pm \sqrt{2}g$, respectively, and the modes of c_{\pm} are highly suppressed, which indicates the information cannot be populated in the state $|e\rangle_3$ of q_3 . Here c , c_- , and c_+ are three normal composite-particle operators.

If we take the initial states of the system with the Hamiltonian H_{eff}^{cp} are $|g\rangle_1 |g\rangle_2 |0\rangle_c$, $|g\rangle_1 |e\rangle_2 |0\rangle_c$, $|e\rangle_1 |g\rangle_2 |0\rangle_c$, and $|e\rangle_1 |e\rangle_2 |0\rangle_c$, respectively, the evolutions of the system can be expressed as

$$|\Psi_1(t)\rangle = e^{-iH_{eff}^{cp} t} |g\rangle_1 |g\rangle_2 |0\rangle_c = |g\rangle_1 |g\rangle_2 |0\rangle_c, \quad (4)$$

$$|\Psi_2(t)\rangle = e^{-iH_{eff}^{cp} t} |g\rangle_1 |e\rangle_2 |0\rangle_c = |g\rangle_1 |e\rangle_2 |0\rangle_c, \quad (5)$$

$$\begin{aligned} |\Psi_3(t)\rangle &= e^{-iH_{eff}^{cp} t} |e\rangle_1 |g\rangle_2 |0\rangle_c \\ &= \cos\left(\frac{g_{a,1}^{g,e}}{\sqrt{2}} t\right) |e\rangle_1 |g\rangle_2 |0\rangle_c + \sin\left(\frac{g_{a,1}^{g,e}}{\sqrt{2}} t\right) |g\rangle_1 |g\rangle_2 |1\rangle_c, \end{aligned} \quad (6)$$

$$\begin{aligned}
 |\Psi_4(t)\rangle &= e^{-iH_{eff}^{cp}t} |e\rangle_1 |e\rangle_2 |0\rangle_c \\
 &= \frac{1}{G} \left[(g_{b,2}^{ef})^2 + (g_{a,1}^{g,e})^2 \cos\left(\sqrt{\frac{G}{2}}t\right) \right] |e\rangle_1 |e\rangle_2 |0\rangle_c \\
 &\quad - \frac{g_{a,1}^{g,e} g_{b,2}^{ef}}{G} \left[\cos\left(\sqrt{\frac{G}{2}}t\right) - 1 \right] |g\rangle_1 |f\rangle_2 |0\rangle_c \\
 &\quad + \frac{-ig_{a,1}^{g,e}}{\sqrt{G}} \sin\left(\sqrt{\frac{G}{2}}t\right) |g\rangle_1 |e\rangle_2 |1\rangle_c.
 \end{aligned} \tag{7}$$

Here $G = (g_{a,1}^{g,e})^2 + (g_{b,2}^{ef})^2$. By using these evolutions, we can construct the c-phase gate on q_1 and q_2 . Its principle can be described as follows.

Suppose that the initial state of the system shown in Fig. 1 with the Hamiltonian H_{eff}^{cp} is

$$|\Psi_0^{cp}\rangle = |0\rangle_c \otimes (\cos \theta_1 |g\rangle_1 + \sin \theta_1 |e\rangle_1) \otimes (\cos \theta_2 |g\rangle_2 + \sin \theta_2 |e\rangle_2). \tag{8}$$

Here $|0\rangle_c \equiv |0\rangle_a |0\rangle_b |g\rangle_3$. By evolving the system with $\frac{g_{a,1}^{g,e}}{\sqrt{2}}t = (2k - 1)\pi$ and $\sqrt{\frac{G}{2}}t = 2m\pi$ ($k, m = 1, 2, 3, \dots$), one can keep the states $|g\rangle_1 |g\rangle_2$ and $|g\rangle_1 |e\rangle_2$ unchanged from Eqs. (4) and (5), respectively. Meanwhile, the state $|e\rangle_1 |g\rangle_2$ undergoes an odd number of periods and generates a minus phase from Eq. (6), and the state $|e\rangle_1 |e\rangle_2$ goes through an even number of periods and maintains unchanged from Eq. (7). That is, the system evolves from Eq. (8) into

$$|\Psi_f^{cp}\rangle = |0\rangle_c \otimes (\alpha_1 |g\rangle_1 |g\rangle_2 + \alpha_2 |g\rangle_1 |e\rangle_2 - \alpha_3 |e\rangle_1 |g\rangle_2 + \alpha_4 |e\rangle_1 |e\rangle_2). \tag{9}$$

Here, $\alpha_1 = \cos \theta_1 \cos \theta_2$, $\alpha_2 = \cos \theta_1 \sin \theta_2$, $\alpha_3 = \sin \theta_1 \cos \theta_2$, and $\alpha_4 = \sin \theta_1 \sin \theta_2$. This is just the result of a c-phase gate on q_1 and q_2 , whose matrix reads

$$U_{e,g}^{cp} = \begin{pmatrix} 1 & 0 & 0 & 0 \\ 0 & 1 & 0 & 0 \\ 0 & 0 & -1 & 0 \\ 0 & 0 & 0 & 1 \end{pmatrix} \tag{10}$$

in the basis $\{|g\rangle_1 |g\rangle_2, |g\rangle_1 |e\rangle_2, |e\rangle_1 |g\rangle_2, |e\rangle_1 |e\rangle_2\}$.

Possible experimental implementation and the SC layout. *The performance of our c-phase gate.* To show the fidelity of our c-phase gate on the two distant qutrits q_1 and q_2 , we numerically simulate the fidelity of our c-phase gate with the Hamiltonian H^{cp} of the whole system which contains the following dispersive couplings:

$$H_{1f}^{cp} = g_{a,1}^{ef} \left(a \sigma_{1;ef}^+ e^{i\delta_{a,1}^{ef}t} + a^+ \sigma_{1;ef}^- e^{-i\delta_{a,1}^{ef}t} \right), \tag{11}$$

$$H_{2f}^{cp} = g_{b,2}^{ge} \left(b \sigma_{2;ge}^+ e^{i\delta_{b,2}^{ge}t} + b^+ \sigma_{2;ge}^- e^{-i\delta_{b,2}^{ge}t} \right), \tag{12}$$

$$H_{3f}^{cp} = g_{a,3}^{ef} \left(a \sigma_{3;ef}^+ e^{i\delta_{a,3}^{ef}t} + a^+ \sigma_{3;ef}^- e^{-i\delta_{a,3}^{ef}t} \right), \tag{13}$$

$$H_{4f}^{cp} = g_{b,3}^{ef} \left(b \sigma_{3;ef}^+ e^{i\delta_{b,3}^{ef}t} + b^+ \sigma_{3;ef}^- e^{-i\delta_{b,3}^{ef}t} \right). \tag{14}$$

The dynamics of the system is determined by the master equation

$$\begin{aligned}
\frac{d\rho}{dt} = & -i[H^{cp}, \rho] + \kappa_a D[a]\rho + \kappa_b D[b]\rho \\
& + \sum_{j=1,2,3} \left\{ \gamma_{jg,e} D[\sigma_{jg,e}^-] \rho + \gamma_{je,f} D[\sigma_{je,f}^-] \rho \right. \\
& + \gamma_{je}^\phi (\sigma_{je} \rho \sigma_{je} - \sigma_{je} \rho / 2 - \rho \sigma_{je} / 2) \\
& \left. + \gamma_{jf}^\phi (\sigma_{jf} \rho \sigma_{jf} - \sigma_{jf} \rho / 2 - \rho \sigma_{jf} / 2) \right\}. \quad (15)
\end{aligned}$$

Here, $\kappa_{a,b}$ is the decay rate of the resonator $r_{a,b}$, $\gamma_{jg,e}$ ($\gamma_{je,f}$) and γ_{je}^ϕ (γ_{jf}^ϕ) are the energy relaxation and the dephase rates of the transition $|e\rangle_j \leftrightarrow |g\rangle_j$ ($|f\rangle_j \leftrightarrow |e\rangle_j$) of q_j , respectively. $\sigma_{je} = |e\rangle_j \langle e|$ and $\sigma_{jff} = |f\rangle_j \langle f|$. $D[L]\rho = (2L\rho L^\dagger - L^\dagger L\rho - \rho L^\dagger L)/2$.

Let us define the fidelity of our c-phase gate as^{17,58,81}

$$F_{cp} = \left(\frac{1}{2\pi} \right)^2 \int_0^{2\pi} \int_0^{2\pi} \langle \Psi_{ideal} | \rho(t) | \Psi_{ideal} \rangle d\theta_1 d\theta_2. \quad (16)$$

Here $|\Psi_{ideal}\rangle$ is the final state of a system by using an ideal c-phase gate operation on its initial state $|\Psi_0^{cp}\rangle$ with the effective Hamiltonian H_{eff}^{cp} . $\rho(t)$ is the realistic density operator after our c-phase gate operation on the initial state $|\Psi_0^{cp}\rangle$ with the realistic Hamiltonian H^{cp} in which the coherence time of qubits, decay rates of resonators, and the unwanted influence on qutrits from the unresonant parts should be taken into account. By taking the feasible experimental parameters as $\omega_1^{g,e}/(2\pi) = \omega_2^{e,f}/(2\pi) = \omega_3^{g,e}/(2\pi) = 7.0$ GHz, $\omega_1^{e,f}/(2\pi) = 6.3$ GHz, $\omega_2^{g,e}/(2\pi) = 7.7$ GHz, $\omega_3^{e,f}/(2\pi) = 6.7$ GHz⁸⁴, $\omega_a/(2\pi) = \omega_b/(2\pi) = 7.0$ GHz, $\gamma_{1,2,3;g,e}^{-1} = (\gamma_{1,2,3;g,e}^\phi)^{-1} = (\gamma_{1,2,3;e,f}^\phi)^{-1} = 2\gamma_{1,2,3;e,f}^{-1} = 50 \mu\text{s}$ ⁸⁵, $g_{a,1}^{g,e}/(2\pi) = \frac{g_{a,1}^{e,f}}{2\sqrt{2}\pi} = 8.2$ MHz, $g_{b,2}^{g,e}/(2\pi) = \frac{g_{b,2}^{e,f}}{2\sqrt{2}\pi} = 10$ MHz, $g_{a,3}^{g,e}/(2\pi) = g_{b,3}^{g,e}/(2\pi) = \frac{g_{a,3}^{e,f}}{2\sqrt{2}\pi} = \frac{g_{b,3}^{e,f}}{2\sqrt{2}\pi} = 260$ MHz⁷¹, and $\kappa_a = \kappa_b \equiv \kappa = 50 \mu\text{s}$ ⁴⁴, we numerically simulate the fidelity of our c-phase gate, which can reach 99.5% within 86.3 ns. Here the coupling strengths of q_1 and q_2 are the optimized ones with $k=m=1$.

To show the possible influences from the realistic condition, we give the relation between the fidelity of our c-phase gate and one of the parameters $\gamma_{1,2,3;g,e}$, κ , $g_{a,1}^{g,e}$, and $\delta = \omega_1^{g,e} - \omega_1^{e,f} = \omega_2^{g,e} - \omega_2^{e,f}$, shown in Fig. 2. In Fig. 2(a), the probability of the information populated in the excited state of the CTQ is almost zero, which indicates the assumption that we take q_3 as a two-energy-level qubit for obtaining Eq. (2) is reasonable. This agrees with the relation between the fidelity and the energy relaxation rate $\gamma_{3;g,e}$ of q_3 , shown in Fig. 2(b). Figure 2(c–f) show that the fidelity of the c-phase gate can be enhanced by a longer life time, small coupling strengths, and large anharmonicities δ of q_1 and q_2 . In Fig. 2(e), the fidelity of the gate is enhanced when $g_1^{g,e} = 8.2$ MHz (the operation time of the gate is about 86.3 ns), compared with the one when $g_1^{g,e} = 5$ MHz (the time is about 140.5 ns). In Fig. 2(f), the fidelity of our c-phase gate is reduced largely when the anharmonicity of the CTQs is $\delta = 0.37$ GHz as the transition $|g\rangle_2 \leftrightarrow |e\rangle_2$ of q_2 is resonant with the mode c_+ at this time, which leads to the influence that its excitation cannot be suppressed. In detail, the difference between the effective Hamiltonian H_{eff}^{cp} and the realistic Hamiltonian H^{cp} becomes a large one. The overlap between the final states $|\Psi_{ideal}\rangle$ and $\rho(t)$ obtained by the evolutions with H_{eff}^{cp} and H^{cp} , respectively from the same initial state $|\Psi_0^{cp}\rangle$ is reduced largely.

Application of our c-phase gate in surface code layout. Operations on superconducting qubit cannot perform sufficiently well to let the qubit act as a computational qubit directly with recent techniques and several works are focused on the realization of the surface code on superconducting qubits for fault-tolerant quantum computing. The tolerance of the SC layout to errors allows as high as about 1% error rate of per operation, which is much bigger than 2×10^{-5} error rate of the per operation required in quantum correction code⁸⁰. Qubits in SC code are divided into three types: data qubits, measure-z qubits, and measure-x qubits. Away from the boundaries, each data (measure) qubits interact with four measure (data) qubits. As an application of our c-phase gate on two distant transmon qutrits, we construct a SC layout with a conventional square lattice^{70,80} for fault-tolerant quantum computing on the DTQs in an effective way.

Our setup for the SC layout is shown in Fig. 3(a) in which each blue square represents a transmon qutrit with the 6.2 MHz coupling strength, each red circle is a transmon qutrit with the 5 MHz coupling strength, and each gray triangle means a CTQ. The small strengths are used to avoid the interactions between the idle resonators and DTQs. To discuss the performance of our c-phase gate on nearest DTQs in the layout, we consider a cell of the layout shown in Fig. 3(b). Here, q_1 , r_a , q_3 , r_b , and q_2 are the same as those in our c-phase gate shown in Fig. 1. The couplings between q_1 and r_a , r_b , and r_e are considered

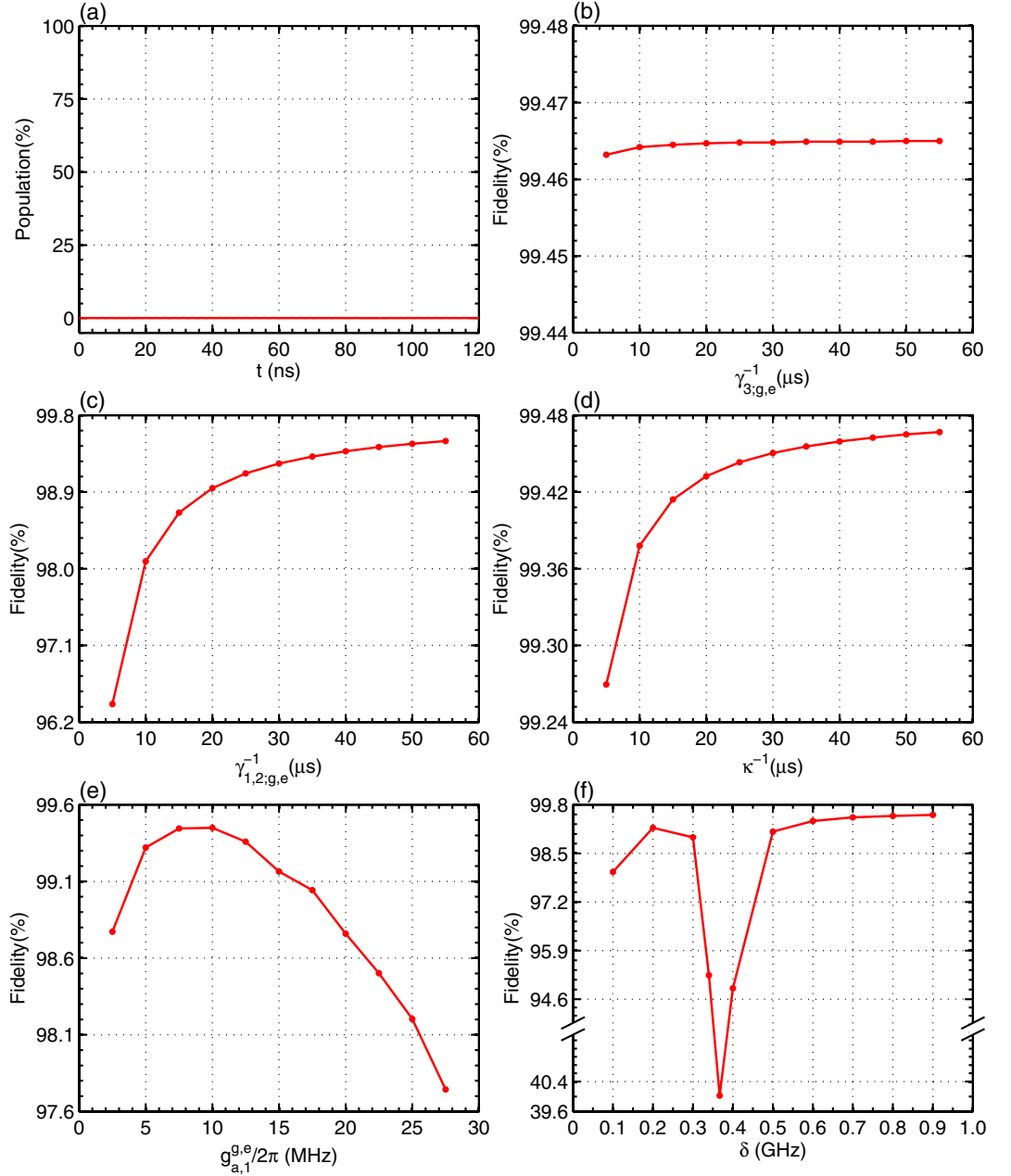


Figure 2. (a) The probability of the information populated in the state $|e_3\rangle$ of q_3 ($|\langle \Psi_0^{cp} | U^{iH^p t} | e_3 \rangle|^2$) during the c-phase gate operation on the maximally entangled state of q_1 and q_2 with $\theta_1 = \theta_2 = \frac{\pi}{2}$ in Eq. (8). (b–f) The fidelity of the c-phase gate on the DTQs q_1 and q_2 varies with $\gamma_{1,2,3,g,e}^{-1}$, κ , $g_{a,1}^{g,e}$, and the anharmonicity of the two transitions of q_1 and q_2 $\delta = \omega_1^{g,e} - \omega_1^{e,f} = \omega_2^{g,e} - \omega_2^{e,f}$.

when the interactions between q_1 and the nearest DTQs are tuned off except for q_2 . The Hamiltonian of the cell is

$$\begin{aligned}
 H^{SC} = & \sum_{I=1,3} \left(g_{a,I}^{g,e} a \sigma_{I;g,e}^+ e^{i\delta_{a,I}^{g,e} t} + g_{a,I}^{e,f} a \sigma_{I;e,f}^+ e^{i\delta_{a,I}^{e,f} t} \right) \\
 & + \sum_{J=2,3} \left(g_{b,J}^{g,e} b \sigma_{J;g,e}^+ e^{i\delta_{b,J}^{g,e} t} + g_{b,J}^{e,f} b \sigma_{J;e,f}^+ e^{i\delta_{b,J}^{e,f} t} \right) \\
 & + \sum_{k=c,d,e} \left(g_{k,1}^{g,e} k \sigma_{1;g,e}^+ e^{i\delta_{k,1}^{g,e} t} + g_{k,1}^{e,f} k \sigma_{1;e,f}^+ e^{i\delta_{k,1}^{e,f} t} \right) + h.c.
 \end{aligned} \tag{17}$$

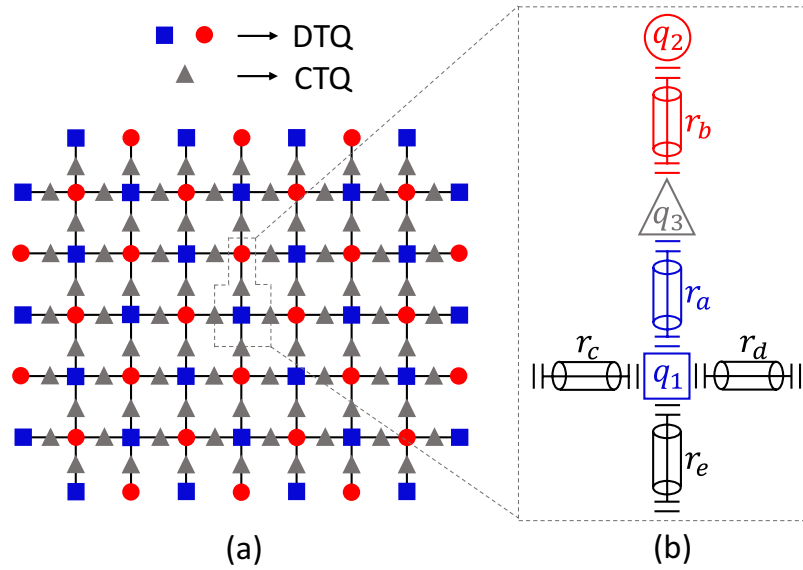


Figure 3. An application of our c-phase gate on two distant transmon qutrits for fault-tolerant quantum computing. (a) The setup for the surface code layout. (b) A cell of the layout.

Here, the frequencies of r_c , r_d , and r_e are taken as 7.5 GHz, 8.0 GHz, and 8.5 GHz, respectively. Except for the coupling strengths which are chosen here as $g_{a,1}^{g,e}/(2\pi) = \frac{g_{a,1}^{e,f}}{2\sqrt{2}\pi} = g_{c,1}^{g,e}/(2\pi) = \frac{g_{c,1}^{e,f}}{2\sqrt{2}\pi} = g_{d,1}^{g,e}/(2\pi) = \frac{g_{d,1}^{e,f}}{2\sqrt{2}\pi} = g_{e,1}^{g,e}/(2\pi) = \frac{g_{e,1}^{e,f}}{2\sqrt{2}\pi} = 5\text{MHz}$ and $g_{b,2}^{g,e}/(2\pi) = \frac{g_{b,2}^{e,f}}{2\sqrt{2}\pi} = 6.2\text{MHz}$, the other parameters are the same as the ones in the construction of our c-phase gate. For simplification, we calculate the fidelity of a cell or our c-phase gate on an initial maximally entangled state as

$$F_{SC} = |\langle \Psi_f^{SC} | e^{-iH^{SC}t} | \Psi^{SC} \rangle|^2,$$

$$F_{cp} = |\langle \Psi_f^{cp} | e^{-iH^{cp}t} | \Psi^{cp} \rangle|^2. \tag{18}$$

Here

$$|\Psi_f^{SC}\rangle = |g\rangle_3 |0\rangle_a |0\rangle_b |0\rangle_c |0\rangle_d |0\rangle_e \otimes (|g\rangle_1 |g\rangle_2 + |g\rangle_1 |e\rangle_2 - |e\rangle_1 |g\rangle_2 + |e\rangle_1 |e\rangle_2), \tag{19}$$

$$|\Psi_f^{cp}\rangle = |g\rangle_3 |0\rangle_a |0\rangle_b \otimes (|g\rangle_1 |g\rangle_2 + |g\rangle_1 |e\rangle_2 - |e\rangle_1 |g\rangle_2 + |e\rangle_1 |e\rangle_2), \tag{20}$$

$$|\Psi^{SC}\rangle = |g\rangle_3 |0\rangle_a |0\rangle_b |0\rangle_c |0\rangle_d |0\rangle_e \otimes (|g\rangle_1 |g\rangle_2 + |g\rangle_1 |e\rangle_2 + |e\rangle_1 |g\rangle_2 + |e\rangle_1 |e\rangle_2), \tag{21}$$

$$|\Psi^{cp}\rangle = |g\rangle_3 |0\rangle_a |0\rangle_b \otimes (|g\rangle_1 |g\rangle_2 + |g\rangle_1 |e\rangle_2 + |e\rangle_1 |g\rangle_2 + |e\rangle_1 |e\rangle_2). \tag{22}$$

The fidelities of both a cell and our c-phase gate on the given initial states change with the time t , shown in Fig. 4 in which we do not consider the decay and the energy relaxation rates of the resonators and the qutrits. One can see that the fidelity of a cell composed of our gate and three additional resonators on the given initial state decreases just a little, compared to that of our c-phase gate. Besides, small coupling strengths of DTQs, a tunable range of 2.5 GHz of a transmon qubit⁸⁶, and a tunable range of 500 MHz within 1 ns⁸⁷ of 1D superconducting resonator allow us to maintain the states of the idle qutrits. That is, our c-phase gate works effectively in the construction of the SC layout for fault-tolerant quantum computing.

In the SC layout for fault-tolerant quantum computing^{70,80}, only the c-phase gate on nearest DTQs are required. Our scheme for the SC layout has some interesting advantages. First, small coupling strengths of DTQs allow us to complete the c-phase gates on nearest DTQs effectively. It can avoid the unwanted interactions from the other transmon qutrits and resonators by choosing proper frequency anharmonicity between a DTQ and its four nearest resonators. Second, CTQs makes the coupling between a pair of DTQs as a four-step one and it can be turned on and off easily. Third, CTQ cannot be excited during the operation of the c-phase gate, and the energy relaxation time of the CTQ has little influence on the fidelity of the gate, which means the tunable-coupling phase qubit with the energy relaxation time of about

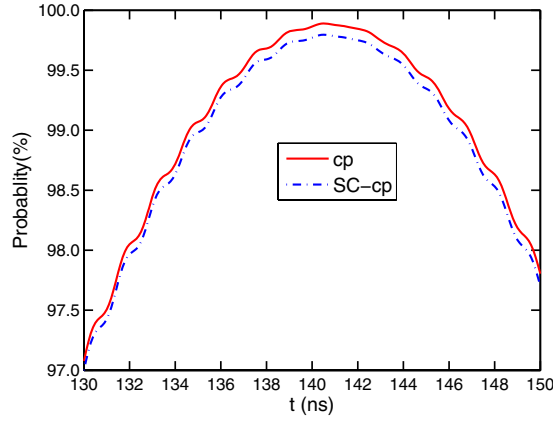


Figure 4. The fidelity of a cell in the surface code layout with our c-phase gate on an initial maximally entangled state of the system composed of q_1 and q_2 , $|\langle \Psi_f^{SC} | e^{-iH^{SC}t} | \Psi \rangle^{SC}|^2$, shown with the blue dash-dotted line. For comparison, the fidelity of our c-phase gate on the same initial state $|\langle \Psi_f^{cp} | e^{-iH^{cp}t} | \Psi \rangle^{cp}|^2$ is given with the red solid line.

130 ns⁸⁸ can also be used here ($100 \text{ MHz} \gg \{6.2, 5.0\} \text{ MHz}$). A tunable regime from 0 MHz to 100 MHz⁸⁸ gives us another way to turn on and off the unwanted interactions from the other DTQs in the layout robustly. All these features make the integration of the layout with a large scale easier.

Conclusion

In conclusion, we have proposed a scheme to construct the c-phase gate on two distant transmon qutrits (q_1 and q_2) which are coupled to different high-quality 1D superconducting resonators (r_a and r_b) intercoupled by a CTQ (q_3) in the resonant regime of $\omega_1^{g,e} = \omega_a = \omega_3^{g,e} = \omega_b = \omega_2^{e,f}$. The gate on distant transmon qutrits has not been studied before. Maybe our scheme can support the solid-state quantum computation based on this device. With our c-phase gate, we have proposed a SC layout for fault-tolerant quantum computing on transmon qutrits, which has attracted much attention^{70,72} as the error rate of quantum gate is hard to be reduced to 10^{-5} with recent techniques. The layout can be divided effectively into some cells by tuning the frequency of CTQs to detune with two nearest resonators largely. It can avoid the interactions from the other parts of the layout and provides a probability for the large scale integration of a SC layout for fault-tolerant quantum computing with circuit QED.

Methods

Hamiltonian and canonical transformations. In the Schrödinger picture, Eq. (2) can be rewritten as

$$\begin{aligned} H_1^{cp} = & \omega_a a^\dagger a + \omega_b b^\dagger b + \omega_1^{g,e} \sigma_{1;g,e}^+ \sigma_{1;g,e}^- + \omega_2^{e,f} \sigma_{2;e,f}^+ \sigma_{2;e,f}^- + \omega_3^{g,e} \sigma_{3;g,e}^+ \sigma_{3;g,e}^- \\ & + g_{a,1}^{g,e} (a \sigma_{1;g,e}^+ + a^\dagger \sigma_{1;g,e}^-) + g_{b,2}^{e,f} (b \sigma_{2;e,f}^+ + b^\dagger \sigma_{2;e,f}^-) \\ & + g_{a,3}^{g,e} (a \sigma_{3;g,e}^+ + a^\dagger \sigma_{3;g,e}^-) + g_{b,3}^{e,f} (b \sigma_{3;g,e}^+ + b^\dagger \sigma_{3;g,e}^-). \end{aligned} \quad (23)$$

Taking the canonical transformations $a = \frac{1}{2}(c_+ + c_- + \sqrt{2}c)$, $b = \frac{1}{2}(c_+ + c_- - \sqrt{2}c)$, and $\sigma_{3;g,e}^- = \frac{\sqrt{2}}{2}(c_+ - c_-)$ with the conditions $\omega_a = \omega_b = \omega_1^{g,e} = \omega_2^{e,f} = \omega_3^{g,e} = \omega$ and $g_{a,3}^{g,e} = g_{b,3}^{e,f} = g$, the Hamiltonian in Eq. (23) can be expressed as

$$\begin{aligned} H = & \omega \sigma_{1;g,e}^+ \sigma_{1;g,e}^- + \omega \sigma_{2;e,f}^+ \sigma_{2;e,f}^- + \omega c^\dagger c + (\omega + \sqrt{2}g) c_+ c_+^\dagger + (\omega - \sqrt{2}g) c_- c_-^\dagger \\ & + \frac{1}{2} [g_{a,1}^{g,e} (c_+ + c_- + \sqrt{2}c) \sigma_{1;g,e}^+ + g_{a,1}^{g,e} (c_+^\dagger + c_-^\dagger + \sqrt{2}c^\dagger) \sigma_{1;g,e}^- \\ & + g_{b,2}^{e,f} (c_+ + c_- - \sqrt{2}c) \sigma_{2;e,f}^+ + g_{b,2}^{e,f} (c_+^\dagger + c_-^\dagger - \sqrt{2}c^\dagger) \sigma_{2;e,f}^-]. \end{aligned} \quad (24)$$

The frequencies of modes c_\pm are $\omega \pm \sqrt{2}g$. When we take $g \gg \{g_{a,1}^{g,e}, g_{b,2}^{e,f}\}$, the excitations of modes c_\pm are highly suppressed as it detunes with the resonance modes (c , q_1 , and q_2 with the frequency of ω) largely, and the Hamiltonian in Eq. (24) can be reduced into

$$H = \omega\sigma_{1;g,e}^+\sigma_{1;g,e}^- + \omega\sigma_{2;e,f}^+\sigma_{2;e,f}^- + \omega c^+c + \frac{1}{\sqrt{2}} \left[g_{a,1}^{g,e} (c\sigma_{1;g,e}^+ + c^+\sigma_{1;g,e}^-) - g_{b,2}^{e,f} (c\sigma_{2;e,f}^+ + c^+\sigma_{2;e,f}^-) \right], \quad (25)$$

which can be written as

$$H = \frac{1}{\sqrt{2}} \left[g_{a,1}^{g,e} (c\sigma_{1;g,e}^+ + c^+\sigma_{1;g,e}^-) - g_{b,2}^{e,f} (c\sigma_{2;e,f}^+ + c^+\sigma_{2;e,f}^-) \right] \quad (26)$$

in the interaction picture.

References

- Nielsen, M. A. & Chuang, I. L. *Quantum Computation and Quantum Information* (Cambridge University, Cambridge, 2000).
- Barenco, A. *et al.* Elementary gates for quantum computation. *Phys. Rev. A* **52**, 3457–3467 (1995).
- Liu, Y., Long, G. L. & Sun, Y. Analytic one-bit and CNOT gate constructions of general n-qubit controlled gates. *Int. J. Quant. Inf.* **06**, 447–462 (2008).
- Feng, G. R., Xu, G. F. & Long, G. L. Experimental realization of nonadiabatic holonomic quantum computation. *Phys. Rev. Lett.* **110**, 190501 (2013).
- Xu, G. & Long, G. Universal nonadiabatic geometric gates in two-qubit decoherence-free subspaces. *Sci. Rep.* **4**, 6814 (2014).
- Xu, G. & Long, G. Protecting geometric gates by dynamical decoupling. *Phys. Rev. A* **90**, 022323 (2014).
- Ren, B. C., Wei, H. R. & Deng, F. G. Deterministic photonic spatial-polarization hyper-controlled-not gate assisted by a quantum dot inside a one-side optical microcavity. *Laser Phys. Lett.* **10**, 095202 (2013).
- Ren, B. C. & Deng, F. G. Hyper-parallel photonic quantum computation with coupled quantum dots. *Sci. Rep.* **4**, 4623 (2014).
- Ren, B. C., Wang, G. Y. & Deng, F. G. Universal hyperparallel hybrid photonic quantum gates with dipole-induced transparency in the weak-coupling regime. *Phys. Rev. A* **91**, 032328 (2015).
- Scully, M. O. & Zubairy, M. S. *Quantum Optics* (Cambridge University, Cambridge, 1997).
- Lukin, M. D. Trapping and manipulating photon states in atomic ensembles. *Rev. Mod. Phys.* **75**, 457 (2003).
- Saffman, M., Walker, T. G. & Mølmer, K. Quantum information with Rydberg atoms. *Rev. Mod. Phys.* **82**, 2313 (2010).
- Su, S. L., Shao, X. Q., Wang, H. F. & Zhang, S. Preparation of three-dimensional entanglement for distant atoms in coupled cavities via atomic spontaneous emission and cavity decay. *Sci. Rep.* **4**, 7566 (2014).
- Li, X. Q. *et al.* An all-optical quantum gate in a semiconductor quantum dot. *Science* **301**, 809 (2003).
- Hu, C. Y. *et al.* Giant optical Faraday rotation induced by a single-electron spin in a quantum dot: Applications to entangling remote spins via a single photon. *Phys. Rev. B* **78**, 085307 (2008).
- Wei, H. R. & Deng, F. G. Universal quantum gates for hybrid systems assisted by quantum dots inside double-sided optical microcavities. *Phys. Rev. A* **87**, 022305 (2013).
- Wei, H. R. & Deng, F. G. Scalable quantum computing based on stationary spin qubits in coupled quantum dots inside double-sided optical microcavities. *Sci. Rep.* **4**, 7551 (2014).
- Togan, E. *et al.* Quantum entanglement between an optical photon and a solid-state spin qubit. *Nature* **466**, 730 (2010).
- Neumann, P. *et al.* Quantum register based on coupled electron spins in a room-temperature solid. *Nat. Phys.* **6**, 249 (2010).
- Yang, W. L. *et al.* One-step implementation of multi-qubit conditional phase gating with nitrogen-vacancy centers coupled to a high-Q silica microsphere cavity. *Appl. Phys. Lett.* **96**, 241113 (2010).
- Wei, H. R. & Deng, F. G. Compact quantum gates on electron-spin qubits assisted by diamond nitrogen-vacancy centers inside cavities. *Phys. Rev. A* **88**, 042323 (2013).
- Wang, C., Zhang, Y., Jiao, R. Z. & Jin, G. S. Universal quantum controlled phase gates on photonic qubits based on nitrogen vacancy centers and microcavity resonators. *Opt. Express* **21**, 19252–19260 (2013).
- Wang, C. *et al.* Complete entanglement analysis on electron spins using quantum dot and microcavity coupled system. *Sci. China-Phys. Mech. Astron.* **56**, 2054–2058 (2013).
- Sheng, Y. B., Liu, J., Zhao, S. Y. & Zhou, L. Multipartite entanglement concentration for nitrogen-vacancy center and microtoroidal resonator system. *Chin. Sci. Bull.* **59**, 3507–3513 (2013).
- Zhou, J. *et al.* High fidelity quantum state transfer in electromechanical systems with intermediate coupling. *Sci. Rep.* **4**, 6237 (2014).
- Lafarge, P. *et al.* Two-electron quantization of the charge on a superconductor. *Nature* **365**, 422 (1993).
- Nakamura, Y., Pashkin, Y. & Tsai, J. S. Coherent control of macroscopic quantum states in a single-Cooper-pair box. *Nature* **398**, 786 (1999).
- Leggett, A. J. & Garg, A. Quantum mechanics versus macroscopic realism: Is the flux there when nobody looks? *Phys. Rev. Lett.* **54**, 857 (1985).
- Mooij, J. E. *et al.* Josephson persistent current qubit. *Science* **285**, 1036 (1999).
- Friedman, J. R. *et al.* Detection of a Schrödinger’s cat state in an rf-SQUID. *Nature* **406**, 43 (2000).
- Ramos, R. C. *et al.* Design for effective thermalization of junctions for quantum coherence. *IEEE Trans. Appl. Supercond.* **11**, 998 (2001).
- Martinis, J. M., Nam, S., Aumentado, J. & Urbina, C. Rabi oscillations in a large Josephson-junction qubit. *Phys. Rev. Lett.* **89**, 117901 (2002).
- Martinis, J. M. Superconducting phase qubits. *Quan. Inf. Process.* **8**, 81 (2009).
- Koch, J. *et al.* Charge-insensitive qubit design derived from the Cooper pair box. *Phys. Rev. A* **76**, 042319 (2007).
- Barends, R. *et al.* Coherent Josephson qubit suitable for scalable quantum integrated circuits. *Phys. Rev. Lett.* **111**, 080502 (2013).
- Rigetti, C. *et al.* Superconducting qubit in a waveguide cavity with a coherence time approaching 0.1 ms. *Phys. Rev. B* **86**, 100506(R) (2012).
- Hood, C. J., Kimble, H. J. & Ye, J. Characterization of high-finesse mirrors: loss, phase shifts, and mode structure in an optical cavity. *Phys. Rev. A* **64**, 033804 (2001).
- Vernooy, D. W. *et al.* Cavity QED with high-Q whispering gallery modes. *Phys. Rev. A* **57**, 2293(R) (1998).
- Armani, D. K., Kippenberg, T. J., Spillane, S. M. & Vahala, K. J. Ultra-high-Q toroid microcavity on a chip. *Nature* **421**, 925 (2003).
- Lev, B. *et al.* Feasibility of detecting single atoms using photonics band gap cavities. *Nanotechnology* **15**, S556 (2004).
- Peng, B. *et al.* Parity-time-symmetric whispering-gallery microcavities. *Nat. Phys.* **10**, 394–398 (2014).

42. Blais, A. *et al.* Cavity quantum electrodynamics for superconducting electrical circuits: An architecture for quantum computation. *Phys. Rev. A* **69**, 062320 (2004).
43. Wallraff, A. *et al.* Strong coupling of a single photon to a superconducting qubit using circuit quantum electrodynamics. *Nature* **431**, 162 (2004).
44. Megrant, A. *et al.* Planar superconducting resonators with internal quality factors above one million. *App. Phys. Lett.* **100**, 113510 (2012).
45. Paik, H. *et al.* Observation of High Coherence in Josephson Junction Qubits Measured in a three-dimensional circuit qed architecture. *Phys. Rev. Lett.* **107**, 240501 (2011).
46. Cleland, A. N. & Roukes, M. L. Fabrication of high frequency nanometer scale mechanical resonators from buck Si crystals. *App. Phys. Lett.* **69**, 2653 (1996).
47. Marquardt, F. & Girvin, S. M. Optomechanics. *Physics* **2**, 40 (2009).
48. Xiang, Z. L., Ashhab, S., You, J. Q. & Nori, F. Hybrid quantum circuits: Superconducting circuits interacting with other quantum systems. *Rev. Mod. Phys.* **85**, 623 (2013).
49. Devoret, M. H. & Schoelkopf, R. J. Superconducting circuits for quantum information: An outlook. *Science* **339**, 1169 (2013).
50. Schuster, D. I. *et al.* Resolving photon number states in a superconducting circuit. *Nature* **445**, 515 (2007).
51. Díaz, P. F. *et al.* Observation of the Bloch-Siegert shift in a qubit-oscillator system in the ultrastrong coupling regime. *Phys. Rev. Lett.* **105**, 237001 (2010).
52. DiCarlo, L. *et al.* Demonstration of two-qubit algorithms with a superconducting quantum processor. *Nature* **460**, 240 (2009).
53. Fedorov, A. *et al.* Implementation of a Toffoli gate with superconducting circuits. *Nature* **481**, 170 (2012).
54. Reed, M. D. *et al.* Realization of three-qubit quantum error correction with superconducting circuits. *Nature* **482**, 382 (2012).
55. Strauch, F. W. All-resonant control of superconducting resonators. *Phys. Rev. Lett.* **109**, 210501 (2012).
56. Yang, C. P., Su, Q. P., Zheng, S. B. & Han, S. Y. Generating entanglement between microwave photons and qubits in multiple cavities coupled by a superconducting qutrit. *Phys. Rev. A* **87**, 022320 (2013).
57. Hua, M., Tao, M. J. & Deng, F. G. Universal quantum gates on microwave photons assisted by circuit quantum electrodynamics. *Phys. Rev. A* **90**, 012328 (2014).
58. Hua, M., Tao, M. J. & Deng, F. G. Fast universal quantum gates on microwave photons with all-resonance operations in circuit QED. *Sci. Rep.* **5**, 9274 (2015).
59. Hua, M., Tao, M. J. & Deng, F. G. Efficient generation of NOON states on two microwave-photon resonators. *Chin. Sci. Bull.* **59**, 2829–2834 (2014).
60. Wang, H. *et al.* Deterministic entanglement of photons in two superconducting microwave resonators. *Phys. Rev. Lett.* **106**, 060401 (2011).
61. Wu, C. W. *et al.* Scalable one-way quantum computer using on-chip resonator qubits. *Phys. Rev. A* **85**, 042301 (2012).
62. Strauch, F. W. Quantum logic gates for superconducting resonator qubits. *Phys. Rev. A* **84**, 052313 (2011).
63. Strauch, F. W., Onyango, D., Jacobs, K. & Simmonds, R. W. Entangled-state synthesis for superconducting resonators. *Phys. Rev. A* **85**, 022335 (2012).
64. Strauch, F. W., Jacobs, K. & Simmonds, R. W. Arbitrary control of entanglement between two superconducting resonators. *Phys. Rev. Lett.* **105**, 050501 (2010).
65. Lucero, E. *et al.* Computing prime factors with a Josephson phase qubit quantum processor. *Nat. Phys.* **8**, 719 (2012).
66. Hu, Y. & Tian, L. Deterministic generation of entangled photons in superconducting resonator arrays. *Phys. Rev. Lett.* **106**, 257002 (2011).
67. Yang, C. P., Su, Q. P. & Nori, F. Entanglement generation and quantum information transfer between spatially-separated qubits in different cavities. *New J. Phys.* **15**, 115003 (2013).
68. Merkel, S. T. & Wilhelm, F. K. Generation and detection of NOON states in superconducting circuits. *New J. Phys.* **12**, 093036 (2010).
69. Jeffrey, E. *et al.* Fast accurate state measurement with superconducting qubits. *Phys. Rev. Lett.* **112**, 190504 (2014).
70. Chow, J. M. *et al.* Implementing a strand of a scalable fault-tolerant quantum computing fabric. *Nat. Commun.* **5**, 4015 (2014).
71. Steffen, L. *et al.* Deterministic quantum teleportation with feed-forward in a solid state system. *Nature* **500**, 319 (2013).
72. Barends, R. *et al.* Superconducting quantum circuits at the surface code threshold for fault tolerance. *Nature* **508**, 500 (2014).
73. Majer, J. *et al.* Coupling superconducting qubits via a cavity bus. *Nature* **449**, 443 (2007).
74. DiCarlo, L. *et al.* Preparation and measurement of three-qubit entanglement in a superconducting circuit. *Nature* **467**, 574 (2010).
75. Hofheinz, M. *et al.* Synthesizing arbitrary quantum states in a superconducting resonator. *Nature* **459**, 546 (2009).
76. Johnson, B. R. *et al.* Quantum non-demolition detection of single microwave photons in a circuit. *Nat. Phys.* **6**, 663 (2010).
77. Wang, H. *et al.* Measurement of the decay of Fock states in a superconducting quantum circuit. *Phys. Rev. Lett.* **101**, 240401 (2008).
78. Hofheinz, M. *et al.* Generation of Fock states in a superconducting quantum circuit. *Nature* **454**, 310 (2008).
79. Dennis, E., Kitaev, A., Landahl, A. & Preskill, J. Topological quantum memory. *J. Math. Phys.* **43**, 4452–4505 (2002).
80. Fowler, A. G., Mariantoni, M., Martinis, J. M. & Cleland, A. N. Surface codes: towards practical large-scale quantum computation. *Phys. Rev. A* **86**, 032324 (2012).
81. Yin, Z. Q. & Li, F. L. Multiatom and resonant interaction scheme for quantum state transfer and logical gates between two remote cavities via an optical fiber. *Phys. Rev. A* **75**, 012324 (2007).
82. Serafini, A., Mancini, S. & Bose, S. Distributed Quantum Computation via Optical Fibers. *Phys. Rev. Lett.* **96**, 010503 (2006).
83. Yang, W. L. *et al.* Entanglement of nitrogen-vacancy-center ensembles using transmission line resonators and a superconducting phase qubit. *Phys. Rev. A* **83**, 022302 (2011).
84. Hoi, I. C. *et al.* Demonstration of a single-photon router in the microwave regime. *Phys. Rev. Lett.* **107**, 073601 (2011).
85. Chang, J. B. *et al.* Improved superconducting qubit coherence using titanium nitride. *App. Phys. Lett.* **103**, 012602 (2013).
86. Schreier, J. A. *et al.* Suppressing charge noise decoherence in superconducting charge qubits. *Phys. Rev. B* **77**, 180502(R) (2008).
87. Wang, Z. L. *et al.* Quantum state characterization of a fast tunable superconducting resonator. *App. Phys. Lett.* **102**, 163503 (2013).
88. Allman, M. S. *et al.* rf-SQUID-mediated coherent tunable coupling between a superconducting phase qubit and a lumped-element resonator. *Phys. Rev. Lett.* **104**, 177004 (2010).

Acknowledgements

GLL was supported by the National Natural Science Foundation of China under Grant Nos. 11175094 and 91221205, and the National Basic Research Program of China under Grant Nos. 2009CB929402 and 2011CB9216002. GLL is a member of the Center of Atomic and Molecular Nanosciences, Tsinghua

University. FGD was supported by the National Natural Science Foundation of China under Grant No. 11474026.

Author Contributions

M.H. and M.J. completed the calculation and prepared the figures. M.H., F.G. and G.L. wrote the main manuscript text. G.L. supervised the whole project. All authors reviewed the manuscript.

Additional Information

Competing financial interests: The authors declare no competing financial interests.

How to cite this article: Hua, M. *et al.* One-step resonant controlled-phase gate on distant transmon qubits in different 1D superconducting resonators. *Sci. Rep.* **5**, 14541; doi: 10.1038/srep14541 (2015).



This work is licensed under a Creative Commons Attribution 4.0 International License. The images or other third party material in this article are included in the article's Creative Commons license, unless indicated otherwise in the credit line; if the material is not included under the Creative Commons license, users will need to obtain permission from the license holder to reproduce the material. To view a copy of this license, visit <http://creativecommons.org/licenses/by/4.0/>